Repetitive Control with Prandtl-Ishlinskii Hysteresis Inverse for Piezo-Based Nanopositioning

Yingfeng Shan and Kam K. Leang[†]
Mechanical Engineering Department
University of Nevada-Reno
Reno, NV 89557-0312 USA

Abstract— **Repetitive control (RC) is a feedback-based approach useful for tracking periodic reference trajectories, for example in scanning applications. The major challenges with RC include closed-loop stability, robustness, and minimizing the steady-state tracking error. In piezo-based nanopositioning systems, the hysteresis effect can limit the performance of RC designed based on a linear dynamics model. An enhanced discrete-time repetitive controller is combined with an inverse-hysteresis compensator based on the Prandtl-Ishlinskii (P-I) model for hysteresis. The feasibility of the inverse model and the performance of the RC system with the inverse compensator are investigated experimentally. Measured results from a flexure-guided nanopositioner show that hysteresis compensation leads to improvement in the stability margin and rate of convergence of the tracking error for the closed-loop RC system. For scanning at 25 Hz, the maximum tracking error is 1.72%.**

I. INTRODUCTION

Repetitive control (RC) is based on the Internal Model Principle [1], where a signal generator is incorporated into a feedback control loop for tracking periodic reference trajectories [2]. This control method is useful in scanning probe microscopes (SPMs), for example in atomic force microscopes (AFMs) [3], where a nanopositioning stage scans the AFM probe in a repetitive fashion relative to a sample surface. Precise tracking of a periodic trajectory is important in applications such as AFM imaging and probe-based nano-pattern generation. However, during positioning the tracking error caused by hysteresis and dynamic effects in the piezoactuator leads to significant positioning error [4]. For operations that are repetitive, the tracking error repeats from one operating cycle to the next and limits the performance of SPMs. Therefore, precise control of the positioning is needed to obtain high-resolution, undistorted images of the sample and for fabricating uniformly distributed patterns of nano-sized features for the growth of novel structures.

The repetitive tracking error in piezo-based nanopositioning systems is addressed by designing an enhanced discrete-time repetitive controller combined with an inverse Prandtl-Ishlinskii (P-I) hysteresis compensator. The inverse P-I compensator minimizes the hysteresis effect to linearize the system for RC implementation; and it also improves the performance of the RC feedback system, where the RC is designed based a linear dynamics model of the piezoactuator. The main contributions include (1) a detailed design of a

discrete-time RC system for AFM, (2) a feasibility study of an inverse P-I model for hysteresis, and (3) the experimental investigation of the closed-loop system's performance.

Repetitive and iteration-based control methods can reduce the tracking error from one operating cycle to the next in nanopositioning systems. For instance, the iterative learning control (ILC) method [5] is effective for minimizing hysteresis and dynamic effects in piezoactuators, and has been widely applied to SPMs [6]. Typically, the ILC method requires resetting the initial conditions at the start of each iteration step. For systems with hysteresis, the input voltage can be cycled (as described in [7]) to re-initialize the system. On the other hand, RC does not require resetting the initial conditions, but the period of the reference trajectory must be known *a priori* [2]. In SPM applications such as imaging and patterning, the reference signal's period is often known in advance. Model-based ILC approaches [5] often require relatively accurate models, and thus add additional challenges in situations where the system dynamics change over time; under cyclic loading [8], for example. The feedback mechanism in RC provides robustness, but the method is most suited for tracking periodic reference trajectories. The RC method has been applied to address run-out issues in disk drive systems [9], [10] and to improve the performance of machine tools [11]. Past work on RC for piezo-based systems and SPMs is limited, but it includes a feedback-linearized controller [12] and a polynomial-based hysteresis inverse compensator [13] combined with RC. Herein, RC is studied for repetitive scanning operations in piezo-based nanopositioning systems where hysteresis is significant.

The major challenges with RC design are stability, robustness, and good steady-state tracking performance. In particular, the effects of hysteresis can lead to poor stability margins [14], and subsequently poor tracking performance. The hysteresis effect is treated as a rate-independent, input nonlinearity and it is characterized by Prandtl-Ishlinkskii model [15], [16], [17]. An inverse compensator based on the P-I model is proposed to minimize the hysteresis effect in piezoactuators for improving the performance of a discrete-time repetitive controller. The RC system is designed based on the linear dynamics model of the piezoactuator; and it incorporates two linear phase compensators for tuning the RC's performance. The control system is experimentally evaluated on a flexure-guided nanopositioner.

[†]Corresponding author; kam@unr.edu; Voice: +1.775.784.7782.

II. AN ENHANCED DISCRETE-TIME REPETITIVE CONTROLLER FOR LINEAR SYSTEMS

Let $R(z)$ be the z transform of a given periodic reference trajectory with period T_p. For tracking such a trajectory, a repetitive controller contains a signal generator with period T_p as shown in Fig. 1(a) [2]. The *plug-in* RC under consideration employs the pure delay z^{-N} in the inner loop to create the signal generator, where $N = T_p/T_s$ and T_s is the sampling period. By '*plug-in*', it is meant that the RC is added to an existing feedback-controlled system, such as a pre-existing PID feedback controller typically used in nanopositioning systems. RC can easily be augmented to an existing feedback controller improved tracking.
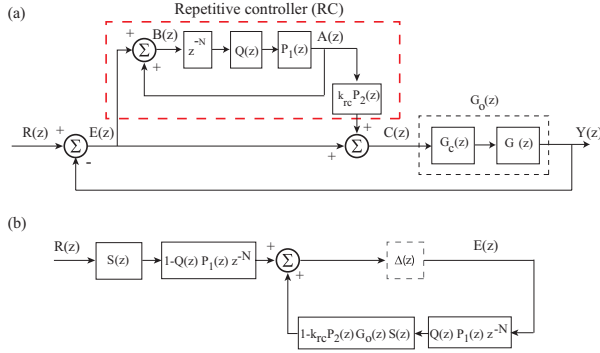
Fig. 1. (a) The block diagram of repetitive control system where the reference trajectory and output are denoted by $R(z)$ and $Y(z)$, respectively. The RC block consists of two linear phase-lead compensators, $P_1(z)$ and $P_2(z)$, to enhance performance. (b) An equivalent block diagram a) for stability analysis, where $E(z)$ is the tracking error.

The input-output dynamics of the positioning system is assumed to be linear and represented by $G(z)$, where $z = e^{j\omega T_s}$, for $\omega \in (0, \pi/T_s)$. (It is pointed out that the input-output behavior of piezo-based nanopositioners consist of hysteresis and dynamic effects. The hysteresis effect will be treated in the next section.) A typical feedback controller is denoted by $G_c(z)$; $Q(z)$ is a low-pass filter for robustness; k_{rc} is the RC gain; and $P_1(z) = z^{m_1}$ and $P_2(z) = z^{m_2}$, where m_1, m_2 are non-negative integers, are positive phase-lead compensators to enhance the performance of the RC feedback system. Particularly, the phase lead compensators z^{m_1} and z^{m_2} are given by $\theta_{1,2}(j\omega) = m_{1,2}T_s$. By inspection, the transfer function of the signal generator that relates $E(z)$ to $A(z)$ in Fig. 1(a) is given by

$$\frac{A(z)}{E(z)} = \frac{Q(z)P_1(z)z^{-N}}{1 - Q(z)P_1(z)z^{-N}} = \frac{Q(z)z^{(-N+m_1)}}{1 - Q(z)z^{(-N+m_1)}}. \quad (1)$$

In the absence of the low-pass filter $Q(z)$ and positive phase lead $P_1(z) = z^{m_1}$, the poles of the signal generator are $1 - z^{-N} = 0$, which implies infinite gain at the harmonics of the periodic reference trajectory. Such large gains are what gives the RC its ability to track periodic trajectories.

Practical RC design incorporates a low-pass filter $Q(z)$ because the large gain at high frequencies can lead to instability of the closed-loop system. For simplicity, a standard low-pass

filter of the form $Q(z) = \frac{a}{z+b}$, where $|a| + |b| = 1$, is chosen. Alternatively, a zero-phase filter can also be used [18].

The stability of the RC system is presented as follows. Let $F(z) = Q(z)z^{(-N+m_1)}$ and $G_0(z) = G_c(z)G(z)$. Consider the following assumptions:

Assumption 1: The reference trajectory $R(z)$ is periodic.

Assumption 2: The closed-loop system without the RC loop is asymptotically stable, *i.e.*, $1 + G_c(z)G(z) = 0$ has no roots outside of the unit circle in the z-plane.

Theorem 1 (Stability of RC): Let Assumption 1 and 2 hold. If $|Q(e^{j\omega T_s})| \leq 1$ for $\omega \in (0, \pi/T_s)$, $1 - F(z)$ is bounded input, bounded output stable, and

$$0 < k_{rc} < \frac{2\cos[\theta_T(\omega) + \theta_2(\omega)]}{A(\omega)}, \quad (2)$$

$$-\pi/2 < [\theta_T(\omega) + \theta_2(\omega)] < \pi/2, \quad (3)$$

then the RC feedback system shown in Fig. 1(a) is asymptotically stable.

Proof: The stability is shown by applying the Small Gain Theorem [19]. First, the transfer function relating the reference trajectory $R(z)$ and the tracking error $E(z)$ is

$$S_{rc}(z) = \frac{E(z)}{R(z)} = \frac{[1 - F(z)]S(z)}{1 - F(z)[1 - k_{rc}P(z)G_0(z)S(z)]}, \quad (4)$$

where $S(z) = 1/(1 + G_0(z))$ is the sensitivity function of the feedback system without the repetitive controller. Furthermore, let $T(z)$ represent the complimentary sensitive function of the closed-loop feedback system without RC, that is, $T(z) = G_0(z)S(z)$. Using Eq. (4), the RC block diagram in Fig. 1(a) is simplified to the equivalent interconnected system shown in Fig. 1(b). Referring to Fig. 1(b), by Assumption 2, $S(z)$ has no poles outside the unit circle in the z-plane, so it is stable. Replacing $z = e^{j\omega T_s}$, and since $1 - F(z)$ stable, the positive feedback closed-loop system in Fig. 1(b) is asymptotically stable when

$$|F(z)[1 - k_{rc}P_2(z)G_0(z)S(z)]| =$$
$$|F(e^{j\omega T_s})[1 - k_{rc}e^{j\theta_2(\omega)}G_0(e^{j\omega T_s})S(e^{j\omega T_s})]| < 1, \quad (5)$$

for all $\omega \in (0, \pi/T_s)$, where the phase lead $\theta_2(\omega) = m_2T_s$.

Noting that $|Q(e^{j\omega T_s})| \leq 1$ and replacing the complimentary sensitive function of the closed-loop system without RC with $T(e^{j\omega T_s}) = A(\omega)e^{j\theta_T(\omega)}$, where $A(\omega) > 0$ and $\theta_T(\omega)$ are the magnitude and phase of $T(e^{j\omega T_s})$, respectively, Eq. (5) can be simplified to

$$|1 - k_{rc}A(\omega)e^{j[\theta_T(\omega) + \theta_2(\omega)]}| < 1. \quad (6)$$

Observing that $e^{j\theta} = \cos(\theta) + j\sin(\theta)$ and $k_{rc} > 0$, Eq. (6) gives

$$-2k_{rc}A(\omega)\cos[\theta_T(\omega) + \theta_2(\omega)] + k_{rc}^2 A^2(\omega) < 0, \quad (7)$$

hence,

$$0 < k_{rc} < \frac{2\cos[\theta_T(\omega) + \theta_2(\omega)]}{A(\omega)} \quad \text{and}$$
$$-\pi/2 < [\theta_T(\omega) + \theta_2(\omega)] < \pi/2.$$

This completes the proof. ∎
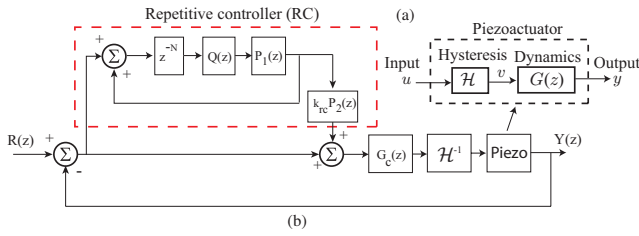
Fig. 2. (a) A cascade model structure for hysteresis and dynamic effects in piezoactuators. The hysteresis is denoted by $\mathcal{H}$, while the linear dynamics is represented by $G(z)$. (b) The modified RC feedback system with an inverse P-I hysteresis compensator $\mathcal{H}^{-1}$ for minimizing hysteresis.

It is noted that the lead compensator $P_1(z)$ compensates for the phase lag caused by the low-pass filter $Q(z)$, and thus can be used to improve the tracking performance [3], [20]. Because $N >> m_1$, the modified delay z^{-N+m_1} is causal and can be easily implemented digitally. Additionally, the lead compensator $P_2(z)$ and RC gain k_{rc} can be adjusted to improve closed-loop robustness and the rate of convergence of the tracking error, respectively.

III. THE PRANDTL-ISHLINSKII HYSTERESIS MODEL FOR FEEDFORWARD COMPENSATION

The design of RC described in the previous section is based on the assumption that the system is linear. In practice, however, the input-output behavior of piezo-based nanopositioning systems exhibits hysteresis and dynamic effects [6]. Hysteresis can affect, for example, closed-loop stability if not accounted for [14]. To enable the application of the proposed RC design, the hysteresis effect is modeled and inverted for feedforward compensation. It is pointed out that charge control can also be used to minimize the hysteresis behavior [21]. However, the model-based approach was preferred over developing a charge control circuit. Specifically, the hysteresis and dynamic effects are described by a cascade model as depicted in Fig. 2(a). The range-dependent hysteresis effect is treated as a rate-independent, input nonlinearity denoted by $\mathcal{H}[\cdot]$. The linear transfer function model $G(z)$ represents the structural (vibrational) dynamics and creep effect [4]. The hysteresis is modeled by the Prandtl-Ishlinskii approach, and an inverse model is developed based on the P-I model structure.

The Prandtl-Ishlinskii model is an operator-type model which has recently been investigated to model hysteresis in piezoactuators [15], [16], [17]. In this model, the output is characterized by the play operator shown in Fig. 3 [15]. Let the input u be continuous and monotone over the interval $t_i \in T_i \triangleq [t_i, t_{i+n}]$, for $n = 1, 2, \cdots, N$. Herein, the play operator $\mathcal{P}_r$ is defined as

$$\mathcal{P}_r[u](0) = p_r(f(0), 0) = 0, \qquad (8)$$
$$\mathcal{P}_r[u](t) = p_r(f(t), p_r[f](t_i)), \qquad (9)$$

where
$$p_r(f(t), p_r[f](t_i)) = \max(f - r, \min(f + r, p_r[f](t_{i-1}))),$$

$f(t) = g_0 u(t) + g_1$ (with g_0, g_1 constants), and $u(t)$ is the input. The play operator's threshold is denoted by r and

three examples are shown in Fig. 3(a). The output $v(t)$ is a weighted sum of play operators,

$$v(t) = \mathcal{H}[u](t) \triangleq k f(t) + \int_0^R d(r) \mathcal{P}_r[u](t) dr, \qquad (10)$$

where k is a positive constant and $d(r)$ is density function that affects the shape and size of the hysteresis curve. Compared to the Preisach hysteresis model, the P-I model is less computationally demanding to implement and invert for feedforward control. An example hysteresis curve generated from the P-I model for a piezoactuator is shown in Fig. 3(b).
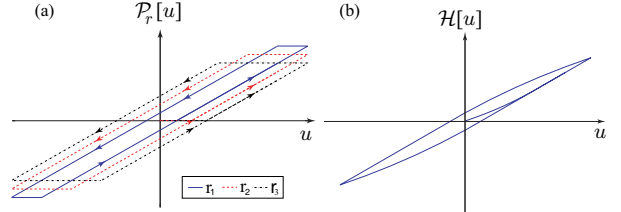
Fig. 3. (a) The play operator with threshold r. (b) The output of the Prandtl-Ishlinskii hysteresis model for a piezoactuator.

An inverse of the P-I model is proposed based on the observation of the shape of the input versus output curve shown in Fig. 4(a) (u vs. v plot). For such a curve, the inverse-play-type operator shown in Fig. 4(b) is proposed for constructing the inverse model.
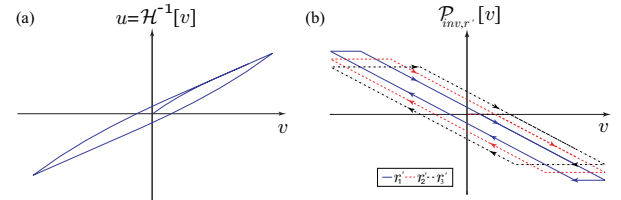
Fig. 4. (a) Input versus measured output plot. (b) A play-type operator for the inverse model with threshold r'.

Therefore, the inverse-play operator shown in Fig. 4(b) is described by

$$\mathcal{P}_{inv,r'}[v](0) = p_{inv,r'}(h(0), 0) = 0,$$
$$\mathcal{P}_{inv,r'}[v](t) = p_{inv,r'}(h(t_i), \mathcal{P}_{inv,r'}[h](t_i)); \qquad (11)$$

where $p_{inv,r'}(h(t), p_{inv,r'}[h](t_i)) = \max(-h - r', \min(-h + r', p_{inv,r'}[h](t_{i-1})))$ and r' denotes the threshold of the inverse-play operator. Then, the output of the inverse hysteresis model is given by

$$\mathcal{H}^{-1}[v](t) \triangleq k_{inv} h(t) + \int_0^R d_{inv}(r') \mathcal{P}_{inv,r'}[v](t) dr'. \quad (12)$$

The function $h(t) = g_0' v(t) + g_1'$, where $v(t)$ is the output of the hysteresis behavior and g_0', g_1' are constants.

IV. EXPERIMENTAL RESULTS

Experiments were done to (1) model the hysteresis behavior and validate the model for a piezoactuator, (2) determine the inverse hysteresis model and apply it for feedforward hysteresis compensation, and (3) combine the inverse hysteresis

model with the proposed repetitive controller for tracking periodic reference trajectories.

A. The Experimental Nanopositioning System

The experimental system is a flexure-guided, serial-kinematic, two-axis nanopositioner optimized for scanning operations with an approximate range of motion of 10 μm $\times$ 10 μm. Figure 5 is a photograph of the scanner and the details of the scanner are found in [22]. Simulation and experimental results are presented for the fast scanning axis (x-direction). A linear dynamics model $G(z)$ of the stack-piezoactuator was obtained for RC design and simulation.
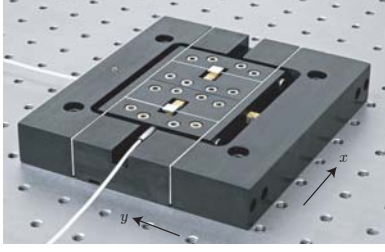
Fig. 5.   Experimental piezo-based nanopositioner [22].

B. Hysteresis Modeling

The coefficients of the forward and inverse models can be determined using input-output data. First, the density function is given by $d(r) = \lambda e^{-\delta r}$, where the threshold values are $r = \rho j$, for $j = 1, 2, \cdots, n$ and the parameters λ, δ, ρ, k are constants. Finally, eight play operators were chosen ($n = 8$), and the parameters $g_0, g_1, \lambda, \delta, \rho, k$ were obtained by curve fitting the measured input-output response from the piezoactuator using the nonlinear least-square optimization toolbox in Matlab.

For example, the output displacement of the piezoactuator was measured by sending a triangle input signal $u(t)$ to the piezo-amplifier. The amplitude was 2 V for seven cycles, then the amplitude was decreased to zero after two cycles. The frequency of the input was 1 Hz to avoid exciting the positioner's resonances. The range of motion was approximately 10 μm. Then the parameters of the hysteresis model were computed from the measured input-output data using the Matlab optimization toolbox. The parameters are $g_0 = 0.7938$, $g_1 = 0.0295$, $\lambda = 0.0211$, $\delta = -6.2904$, $\rho = 0.0919$, and $k = 1$.

The measured and model outputs are compared in Fig. 6, where the inset figure shows the hysteresis curves. The results show good agreement between the measured and model output, where the maximum error was less than 2.5% of the total range. To validate the cascade model structure shown in Fig. 2(a), experiments and simulation results are compared for ± 4 μm range of motion at 1, 10, 25 Hz scanning as shown in Fig. 7, plots (a1) through (c2). The maximum tracking error over one period of the triangle scan is less than 2% as indicated in plots (a2), (b2), and (c2). The accuracy of the cascade model for a 100 Hz sinusoidal scanning motion is shown in Fig. 7(d1) and (d2), where the maximum error is less than 2.5% between the model and measured response.
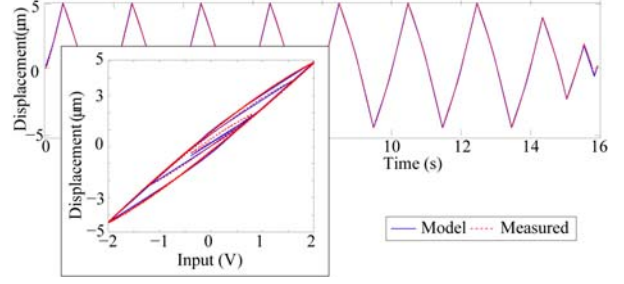
Fig. 6.   Comparison of measured hysteresis and P-I hysteresis model output.
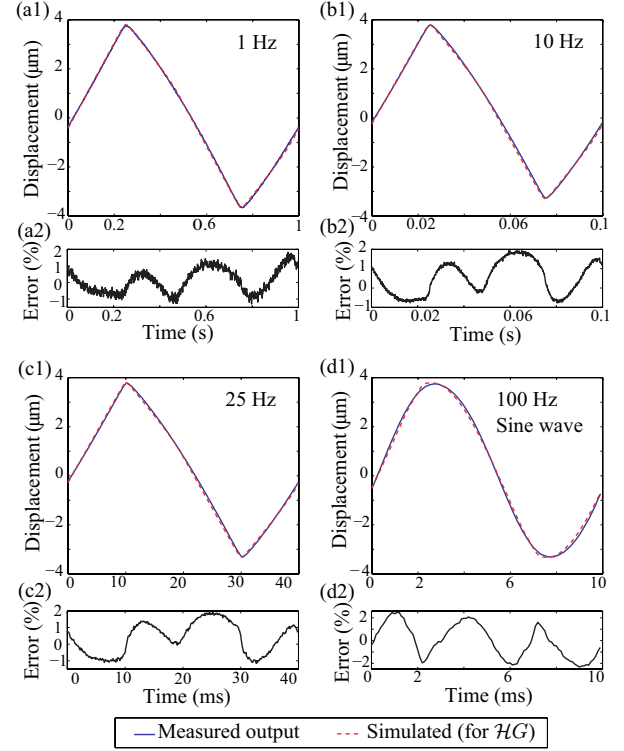
Fig. 7.   Experimental validation of cascade P-I hysteresis $\mathcal{H}$ and linear dynamics $G(z)$ model. (a1) and (a2) Displacement and error vs. time between measured (solid line) and model output (dash line) at 1 Hz (triangle trajectory); (b1) and (b2) the comparison for 10 Hz scanning; (c1) and (c2) the comparison for 25 Hz scanning; and (d1) and (d2) the comparison of sinusoidal scanning at 100 Hz.

C. Inversion-Based Hysteresis Compensation

The hysteresis effect was compensated for using the proposed P-I inverse hysteresis model. The inverse model was obtained using the measured input-output data from the forward model. The density function was chosen as $d_{inv}(r') = \lambda' e^{-\delta' r'}$, where r' is the threshold of the inverse-play operator. Similar to the forward model, the threshold values are given by $r' = \rho' j$, for $j = 1, 2, \cdots, 8$, and the parameters $\lambda', \delta', \rho', k'$ are real constants. Using the measured input-output data, the parameters of the inverse model were found using the nonlinear least-square optimization toolbox in Matlab. The values are $g_0' = 1.1435$, $g_1' = -0.2900$, $\lambda' = 0.0211$, $\delta' = -1.766$, $\rho' = 0.526$, and $k' = 1$.

The results of the inversion-based feedforward controller minimizing hysteresis are shown in Fig. 8. The computed inverse model is depicted in Fig. 8(a). A comparison of the hysteresis curves with (solid line) and without (dash
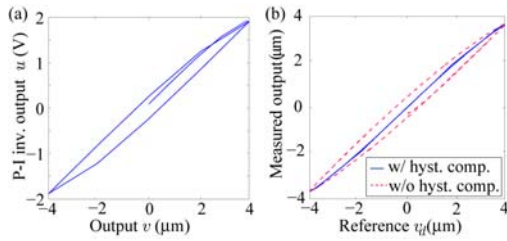
Fig. 8. (a) Inverse hysteresis model. (b) The hysteresis curves for the piezoactuator with (solid line) and without (dash line) feedforward compensation.
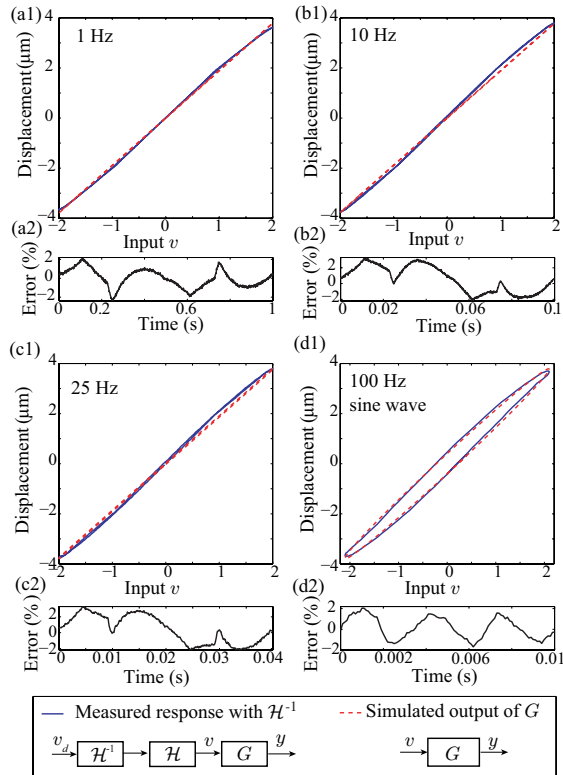
Fig. 9. Validating cascade model by compensating for hysteresis. Comparison of output vs. input plots and error for: (a1) and (a2) 1 Hz triangular trajectory; (b1) and (b2) 10 Hz triangular trajectory; (c1) and (c2) 25 Hz triangular trajectory; and (d1) and (d2) 100 Hz sinusoidal trajectory.

line) feedforward compensation is shown in Fig. 8(b). It can be seen that the inversion-based feedforward controller minimizes the hysteresis behavior, subsequently linearizing the piezoactuator's response.

To further validate the cascade model structure, as well as the quality of the inverse model, the feedforward controller was applied to compensate for hysteresis over different frequency ranges. By compensating for hysteresis, the measured response is dominated by the dynamic effects $G(z)$ [see Fig. 2(a)]. Figure 9 shows the measured and simulated outputs versus input plots for a triangle scan profile at 1, 10, 25 Hz and a 100 Hz sinusoidal trajectory. The maximum error is less than 2.5% and 2% for 25 Hz and 100 Hz, respectively. The results show that the hysteresis effect can be compensated for using the proposed inverse model, thus linearizing the piezoactuator's response.

D. Closed-Loop Stability Evaluation

Hysteresis and its effect on closed-loop stability was experimentally evaluated and compared to simulation results before implementing the repetitive controller. A PID controller was designed based on the linear dynamics model $G(z)$. The controller transfer function is given by $G_c(z) = K_p + K_i \left(\frac{z}{z-1} \right) + K_d \left(\frac{z-1}{z} \right)$, where the Ziegler-Nichols method was used to tune the controller parameters to $K_p = 8.5$, $K_i = 1$, and $K_d = 4$.

The simulated results of the effect of hysteresis on the performance of the PID-controlled system is shown in Fig. 10(a1) and (a2). It can be seen that for a stable PID controller designed based on the linear model, introducing hysteresis effect (using the P-I model) causes the performance of the controller to deteriorate. The tracking results in Fig. 10(a1) and (a2) show oscillations in the response for tracking a 25 Hz triangle trajectory. As shown in simulation, incorporating the P-I inverse model the stability is recovered [dash line in Fig. 10(a1) and (a2)].
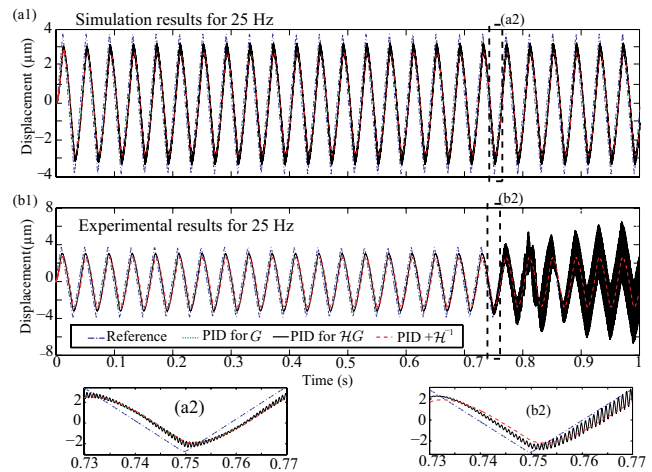
Fig. 10. The effect of hysteresis on the closed-loop stability for tracking 25 Hz triangle trajectory. (a1) and (a2) simulation results comparing PID control of the linear dynamics $G(z)$ (dotted line); PID control of the hysteresis $\mathcal{H}$ and dynamics $G(z)$ model (solid line); and PID combined with $\mathcal{H}^{-1}$ controller (dash line). (b1) and (b2) experimental results.

Experimental results confirm that hysteresis leads to low stability margins as shown in Fig. 10(b1) and (b2). The closed-loop system's error becomes appreciably large at approximately 0.75 s, and is unstable. By integrating the P-I inverse to account for the hysteresis, stability is achieved and the performance of the experimental system matches the simulated response of the PID for the linear dynamics. Therefore, it is evident from the experimental results that hysteresis leads to low stability margin and can make the closed-loop system unstable when a PID controller is designed based on a linear model.

E. Tracking Results of RC with Hysteresis Compensation

In this experiment, the PID and feedforward hysteresis compensator were combined with the proposed RC controller. The repetitive controller was designed based on the linear dynamic model $G(z)$ of piezoactuator as described in Section II. The PID gains were tuned for the piezoactuator

system, where $K_p = 1$, $K_i = 1$, and $K_d = 4$. The RC gain was selected as $k_{rc} = 1.5$ [satisfying condition (2)] and the two phase lead compensators z^{m_1} and z^{m_2} were chosen as $m_1 = 6$ and $m_2 = 0$. The cut-off frequency for the low-pass filter $Q(z)$ was 250 Hz. The RC, PID, and P-I inverse compensator were implemented using Matlab's xPC Target environment with a sampling frequency of 10 kHz.

The tracking error versus time results are shown in Fig. 11, plots (a), (b), and (c), and error measures are listed in Table I. Triangle reference trajectories at 5, 10, and 25 Hz were applied to the control system. As shown, by integrating the hysteresis compensator, the maximum tracking error of the PID controller is reduced from 14.89% to 9.17% at 25 Hz. Simply using PID with RC, the tracking error is further reduced to 2.19% at 25 Hz. Finally, the addition of the hysteresis compensator lowers the maximum tracking to 1.72%. One advantage of the hysteresis compensator is the tracking error of the closed-loop system converges approximately 40% faster, from 0.35 s compared to 0.2 s as shown in Fig. 11(c). The measured steady-state displacement vs. time for the piezoactuator in Fig. 11(d) shows good tracking performance for the overall closed-loop system for tracking a periodic triangle reference trajectory.
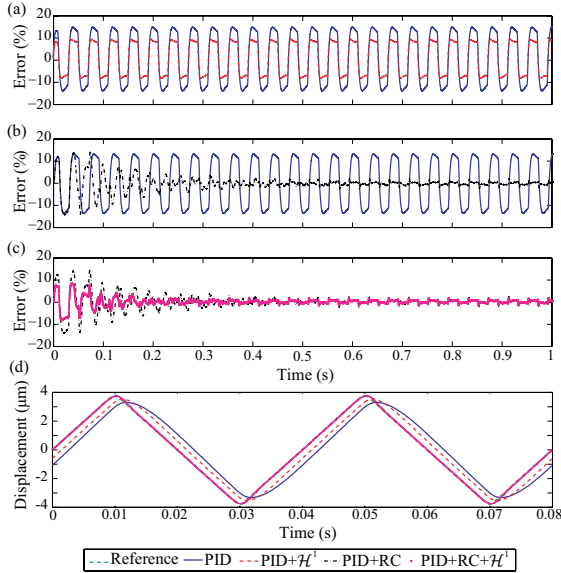
Fig. 11. Experimentally measured tracking error comparing (a) PID with and without $\mathcal{H}^{-1}$; (b) PID and RC (without $\mathcal{H}^{-1}$); (c) PID+RC and PID+RC+$\mathcal{H}^{-1}$; and (d) snapshot of steady-state displacement vs. time.

TABLE I

TRACKING ERROR REPORTED AS PERCENTAGE OF TOTAL RANGE.

Controller	5 Hz		10 Hz		25 Hz	
	e_{max}	e_{rms}	e_{max}	e_{rms}	e_{max}	e_{rms}
PID	3.54	2.67	6.63	5.43	14.89	14.29
PID+$\mathcal{H}^{-1}$	2.28	1.61	4.07	3.25	9.17	8.38
PID+RC	0.46	0.14	0.73	0.23	2.19	0.79
PID+RC+$\mathcal{H}^{-1}$	0.42	0.13	0.62	0.22	1.72	0.68

V. CONCLUSIONS

A discrete-time repetitive controller was designed based on a linear dynamics model of the piezoactuator. The hysteresis effect was modeled by the Prandtl-Ishlinskii method and an inverse compensator was proposed to minimize the hysteresis effect. Experimental results showed good tracking performance for the closed-loop system where at 25 Hz scanning, the maximum tracking error was 1.72%.

REFERENCES

[1] B. A. Francis and W. M. Wonham, "The internal model principle of control theory," *Automatica*, vol. 12, no. 5, pp. 457 – 465, 1976.
[2] T. Inoue, M. Nakano, and S. lwai, "High accuracy control of a proton synchrotron magnet power supply," in *Proc. 8thWorld Congr. IFAC*, 1981, pp. 216 – 221.
[3] U. Aridogan, Y. Shan, and K. K. Leang, "Discrete-time phase compensated repetitive control for piezoactuators in scanning probe microscopes," in *ASME Dynamic Systems and Control Conference*, Ann Arbor, Michigan, 2008, pp. DSCC2008–2283.
[4] D. Croft, G. Shed, and S. Devasia, "Creep, hysteresis, and vibration compensation for piezoactuators: atomic force microscopy application," *ASME J. Dyn. Syst., Meas., and Control*, vol. 123, pp. 35–43, 2001.
[5] Y. Wu and Q. Zou, "Iterative control approach to compensate for both the hysteresis and the dynamics effects of piezo actuators," *IEEE Control Systems Technology*, vol. 15, no. 5, pp. 936 – 944, 2007.
[6] K. K. Leang, Q. Zou, and S. Devasia, "Feedforward control of piezoactuators in atomic force microscope systems: inversion-based compensation for dynamics and hysteresis," *IEEE Cont. Syst. Mag.*, vol. 29, no. 1, pp. 70 – 82, 2009.
[7] K. K. Leang and S. Devasia, "Design of hysteresis-compensating iterative learning control for piezo positioners: application to atomic force microscopes," *Mechatronics*, vol. 16, no. 3–4, pp. 141 – 158, 2006.
[8] M. D. Hill, G. S. White, C.-S. Hwang, and I. K. Lloyd, "Cyclic damage in lead zirconate titanate," *J. Am. Ceram. Soc.*, vol. 79, no. 7, pp. 1915 – 1920, 1996.
[9] K. K. Chew and M. Tomizuka, "Digital control of repetitive errors in disk drive systems," *IEEE Cont. Syst. Mag.*, vol. 10, no. 1, pp. 16 – 20, 1990.
[10] M. Steinbuch, S. Weiland, and T. Singh, "Design of noise and period-time robust high-order repetitive control, with application to optical storage," *Automatica*, vol. 43, no. 12, pp. 2086 – 2095, 2007.
[11] S.-L. Chen and T.-H. Hsieh, "Repetitive control design and implementation for linear motor machine tool," *International Journal of Machine Tools & Manufacture*, vol. 47, no. 12–13, pp. 1807 – 1816, 2007.
[12] G. S. Choi, Y. A. Lim, and G. H. Choi, "Tracking position control of piezoelectric actuators for periodic reference inputs," *Mechatronics*, vol. 12, no. 5, pp. 669–684, 2002.
[13] H.-S. Ahn, "Design of a repetitive control system for a piezoelectric actuator based on the inverse hysteresis model," in *The Fourth International Conference on Control and Automation*, Montreal, Canada, 2003, pp. 128 – 132.
[14] J. A. Main and E. Garcia, "Piezoelectric stack actuators and control system design: strategies and pitfalls," *AIAA J. Guidance, Control, and Dynamics*, vol. 20, no. 3, pp. 479–485, 1997.
[15] M. Brokate and J. Sprekels, *Hysteresis and phase transitions*. New York: Springer, 1996.
[16] K. Kuhnen, "Modeling, identification and compensation of complex hysteretic nonlinearities: a modified prandtl-ishlinskii approach," *European Journal of Control*, vol. 9, no. 4, pp. 407 – 418, 2003.
[17] M. A. Janaideh, C.-Y. Su, and S. Rakheja, "Development of the rate-dependent prandtl-ishlinskii model for smart actuators," *Smart Mater. Struct.*, vol. 17, p. 035026 (11pp), 2008.
[18] M. Tomizuka, "Zero phase tracking algorithm for digital control," *ASME J. Dyn. Syst. Meas. and Cont.*, vol. 109, pp. 65 – 68, 1987.
[19] K. Zhou and J. C. Doyle, *Essentials of robust control*. Prentice-Hall, Inc., 1998.
[20] H. L. Broberg and R. G. Molyet, "A new approach to phase cancellation in repetitive control," in *IEEE Industry Applications Society Annual Meeting*, vol. 3, 1994, pp. 1766 – 1770.
[21] A. J. Fleming and K. K. Leang, "Evaluation of charge drives for scanning probe microscope positioning stages," in *American Control Conference*, Seattle, WA, USA, 2008, pp. 2028 – 2033.
[22] K. K. Leang and A. J. Fleming, "High-speed serial-kinematic AFM scanner: design and drive considerations," *Asian Journal of Control (in Press)*, 2009.